

Diffuse OH in the milky way

M.D. Gray

Dept. of Physics, UMIST, P.O. Box 88, Manchester, M60 1QD, U.K.

M.R.W. Masheder

Dept. of Physics, University of Bristol, Tyndall Avenue, Bristol, BS8 1TL, U.K.

Abstract. We obtain integrated gains for the OH ground-state lines from an exact radiation transfer code with parameters suitable for a large molecular cloud. Results show that the lines are usually formed in NLTE, and that the satellite lines typically show conjugate behaviour. Constraints are set on the OH abundance and kinetic temperature by the requirement that there be no strong maser emission in the main lines.

1. Introduction

OH maser emission is a familiar feature of high-mass star-forming regions in the Milky Way, and also in other source types, for example the circumstellar envelopes of AGB and post-AGB stars. However, it is also possible to observe the spectra of a much more diffuse distribution of OH, associated with Galactic molecular cloud complexes. The bright maser features appear on much smaller angular scales, usually associated with the presence of uCHII regions.

Observations indicate that the spectral signature of the diffuse OH is a combination of emission and absorption, with the emission largely confined to the satellite lines. There is also evidence that the diffuse OH spectra are not generated under LTE conditions. This work describes an attempt to model the diffuse OH emission and absorption via a non-LTE radiation transfer code, based on the accelerated lambda iteration (ALI) method.

2. Observations

Spectra of diffuse OH emission and absorption at all four ground-state frequencies were taken by Dr M.R.W. Masheder using the Dwingeloo telescope. These observations were made along many lines of sight close to the Galactic plane, mostly associated with IRAS point sources. A typical set of spectra is shown in Figure 1.

Observations in the Southern Hemisphere were carried out by Brooks & Whiteoak (2001). These observations were made towards NGC6334, a star-forming complex 1.7 kpc away in the Sagittarius arm, using the ATNF Compact Array, so images as well as spectra were produced. In addition to the ground-

state OH lines, the continuum at 1.6 GHz was also imaged. The beam at 1.6 GHz is $\sim 30'$.

3. Observational Characteristics

If the OH ground state lines were formed in LTE, we expect their optical depths to obey the OH 'sum rule' (for example Rogers & Barrett, 1967) which can be expressed as

$$\tau_{1612} + \tau_{1720} = \frac{\tau_{1665}}{5} + \frac{\tau_{1667}}{9} \quad (1)$$

but the observations rarely obey this rule, indicating NLTE line formation. A second characteristic is that the main lines are typically seen in absorption, whilst the satellite lines exhibit a conjugate behaviour, with emission at 1720 MHz and absorption at 1612 MHz switching to the alternative configuration when critical values of one or more parameters are reached (van Langevelde et al. 1995). This behaviour has been explained as a density effect by Elitzur (1992), who suggests a collisional pump favouring emission at 1720 MHz is replaced by a radiative process, more favourable to emission at 1612 MHz beyond some critical density.

4. The Model

The model is an OH-specific version of the MULTIMOL code (Jones et al. 1994) developed from an original ALI code by Scharmer & Carlsson (1985). The cloud is modelled as a slab, with a standard thickness of 30 pc, which compares well with the 15 pc spanned by the Compact Array beam (see Section xx). The NLTE solutions are exact within the confines of the slab geometry. The model calculates molecular energy-level populations, n_k , for the k -th level, at various depths, within the model. These may be converted to optical depth to compare with observations via the formula:

$$\tau_{ji} = \frac{A_{ji}}{4\pi\Delta\nu} \left(\frac{\ln 2}{\pi}\right)^{1/2} \left(\frac{c}{\nu}\right)^3 \int_0^L dl [n_i - (g_i/g_j)n_j] \quad (2)$$

where A_{ji} is the Einstein A-coefficient of the transition, frequency ν , between upper level j , and lower level i . The line width at FWHM is $\Delta\nu$, and L is the total cloud thickness. For this initial study, only the velocity has been allowed to vary through the cloud (function of l) whilst the density, OH abundance, kinetic and dust temperatures are fixed for all l , but may be varied between program runs.

5. Conjugate Behaviour

In Figure 1, Figure 2 and Figure 3, there is clear evidence of conjugate behaviour in the satellite lines, with one often inverted when the other is absorbing, see also van Langevelde et al. (1995). However, it can be seen that the velocity shift, which controls FIR overlap pumping is important in controlling this behaviour as well as OH abundance.

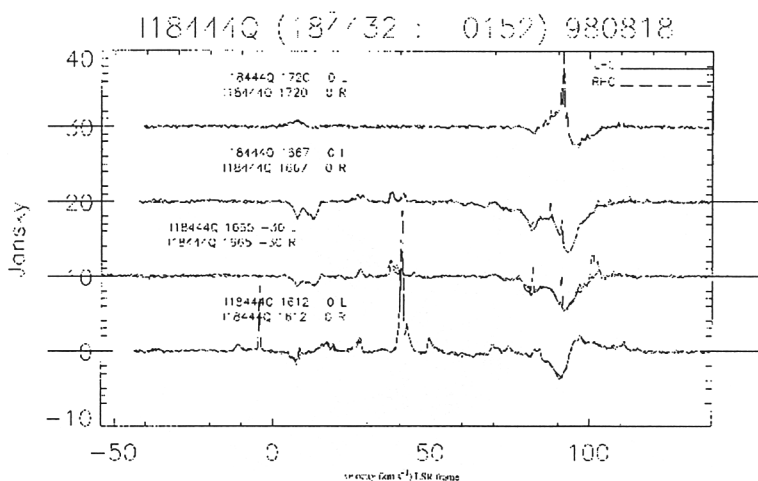


Figure 1. A sample spectrum of diffuse Galactic OH in the four ground state lines and both hands of polarization

6. Discussion

In Figure 2, we plot the negative of the optical depth of the OH ground state satellite lines for a typical cloud model. The H_2 number density for this model is 1000 cm^{-3} and the velocity shift is -40.0 km s^{-1} . The OH column is approximately 10^{15} cm^{-2} . Figure 3 shows the main-line behaviour for the same model.

Note that in the near corner, typical of cold molecular clouds, the main lines are in absorption, as observed, whilst one of the satellite lines (1720 MHz) is in emission. At higher temperatures and OH abundances, the 1667 MHz main line becomes inverted, and we move towards the star-forming maser conditions, characterized by the hotter, denser regions found near to uCHII regions. We can therefore be sure that the diffuse OH exists in conditions colder than about 30 K, and OH abundance $< 5 \times 10^{-8}$ relative to H_2 . It is also possible to use the model to produce synthetic spectra.

References

- Rogers, A. E., & Barrett, A. H. 1967 in IAU31 Conf. Proc., Radio Astronomy and the Galactic System, ed. H. van Woerden, (London: Academic Press)
- Brooks, K. J., & Whiteoak, J. B. 2001, MNRAS, 320, 465
- Elitzur, M. 1992, Astronomical Masers, (Dordrecht: Kluwer)
- van Langevelde, H. J., van Dishoeck, E. F., Sevenster, M. N., & Israel, F. P. 1995, ApJ, 448, L123
- Jones, K. N., Field, D., Gray M. D., & Walker R. N. F. 1994, A&A, 288, 581
- Scharmer G. B., & Carlsson M. 1985, J. Comp. Phys., 59, 56

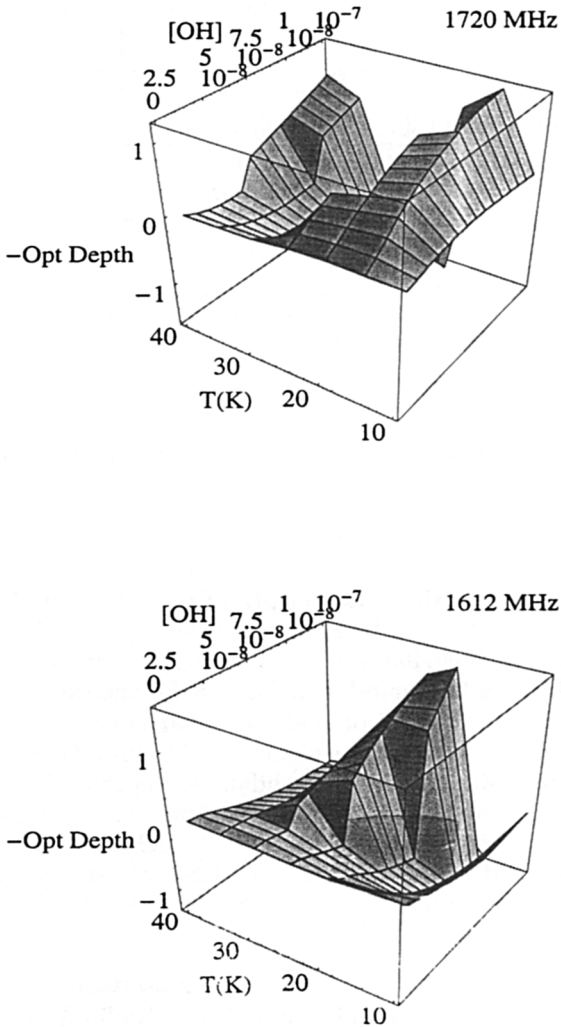


Figure 2. Integrated gains (negative optical depths) in the OH satellite lines at emergent line centre for a model with a velocity shift of 40 km s^{-1} across the cloud.

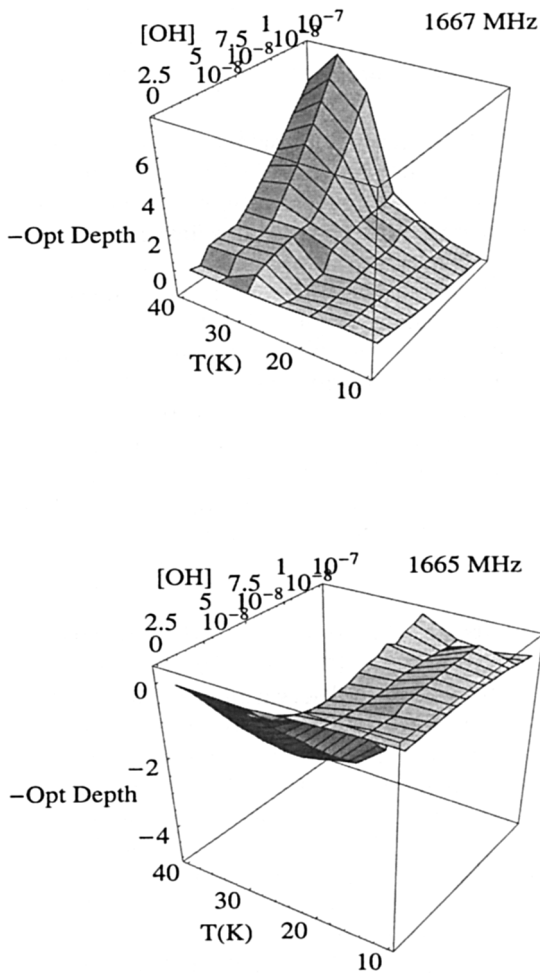


Figure 3. Integrated gains (negative optical depths) in the OH main lines at emergent line centre for a model with a velocity shift of 40 km s^{-1} across the cloud.